



Assessment of uncertainties in projected temperature and precipitation over the Arabian Peninsula: a comparison between different categories of CMIP3 models

Mansour Almazroui¹ · Sajjad Saeed^{1,2} · M. Nazrul Islam¹ · M. Salman Khalid¹ ·
Abdulrahman K. Alkhalaf¹ · Ramzah Dambul¹

Received: 1 February 2017 / Accepted: 3 August 2017 / Published online: 12 September 2017
© The Author(s) 2017, corrected publication September 2017. This article is an open access publication

Abstract

Background This paper examined the level of uncertainties in precipitation and temperature simulations by Coupled Model Intercomparison Project Phase 3 (CMIP3) over the Arabian Peninsula.

Purpose Different techniques are employed to assess the ranges of uncertainties in projected temperature and precipitation over the Arabian Peninsula.

Methods For the present climate (1970–1999), the 22 CMIP3 models are grouped into four out of which two main categories, i) all models ensemble and ii) best performing models ensemble, are used to assess the uncertainties in the future temperature and precipitation over the Arabian Peninsula.

Results The CMIP3 ensemble projections for the above two main categories revealed a continuous increase in temperature over the peninsula during the 21st century. For the period 2070–2099, the all (best performing) models ensemble revealed an increase in temperature by 2.32 ± 2.45 (3.85 ± 1.54), 3.49 ± 2.49 (4.91 ± 1.61), and 3.82 ± 1.47 (5.36 ± 1.47) °C, relative to the present climate, under the B1, A1B, and A2 scenario, respectively, while the intermodel

ranges are projected to be from -3.36 to 6.08 (0.84 to 5.96), -2.26 to 7.68 (1.94 to 7.29), and -1.79 to 7.40 (2.75 to 7.10) °C, respectively. Meanwhile, for the same period, the annual precipitation is projected to increase by 5.16 ± 30 (3.2 ± 25), 10.48 ± 34 (1.82 ± 28), and 15.29 ± 43 (5.3 ± 32)%, relative to the present climate under the B1, A1B, and A2 scenario, while the intermodel ranges are projected to be from -94 to 265 (-71 to 175), -95 to 322 (-74 to 205), and -95 to 375 (-75 to 235)%, respectively, for all (best performing) models ensemble.

Conclusion The uncertainty of projected temperature and precipitation is reduced in the best performing models ensemble compared to the all models. At annual scale, surplus (deficit) precipitation pattern is projected across southern and southwestern (northern and northwestern) parts of the peninsula. The above results indicate that a better choice of models from the CMIP3 database could reduce the uncertainty range associated with future projections over the Arabian Peninsula.

Keywords CMIP3 · Climate models · Arabian Peninsula · Temperature and precipitation · Projection · Uncertainty

The original version of this article was revised: modifications have been made to the abstract, in section 3.3, in figure 12 and 15.

Electronic supplementary material The online version of this article (doi:10.1007/s41748-017-0012-z) contains supplementary material, which is available to authorized users.

✉ Mansour Almazroui
mansour@kau.edu.sa

¹ Center of Excellence for Climate Change Research/
Department of Meteorology, King Abdulaziz University,
P.O. Box 80234, Jeddah 21589, Saudi Arabia

² Department of Earth and Environmental Sciences, KU
Leuven, Louvain, Belgium

1 Introduction

The data set produced in the third phase of the Coupled Model Intercomparison Project (CMIP) formally known as CMIP3 data set (Meehl et al. 2007) has been widely used by the climate scientists to examine the potential future climate conditions all over the globe. Until now, there are more than 600 published documents available on different climatic issues using CMIP3 data set. A list of the publications using CMIP3 data set is available on http://www-pcmdi.llnl.gov/ipcc/subproject_publications.php. Among

them, only one study addresses the potential future climate scenarios over the Arabian Peninsula using the CMIP3 data set (Almazroui et al. 2016). The previous studies (e.g., Almazroui et al. 2013, Barfus and Bernhofer 2014) examined the performance of CMIP3 models over the Arabian Peninsula in the present day climate. Some other studies also provided insight into recent climate change and extremes over the Arabian Peninsula (e.g., Almazroui et al. 2012a, b; Deng et al. 2015; Donat et al. 2014; El Kenawy et al. 2014; AlSarmi and Washington 2011, 2013, Kwarteng et al. 2009; Evans 2009). However, a comprehensive analysis of the uncertainties associated with future projections over the Arabian Peninsula for different categories of CMIP3 models including well performing models compared to the observations is missing in the literature.

The Arabian Peninsula has been neglected in the climate change research compared to the other areas in the world. The international initiatives made by Intergovernmental Panel on Climate Change (IPCC) have placed the Arabian Peninsula at the edge of Asian and African regions, and hence, very less information is available to understand the future climate projections and associated uncertainties over this region. The uncertainties in the future projections vary from region to region and model to model and, additionally, depend on various climatic parameters. For examples, over the tropics, the signal-to-noise ratio is lowest for precipitation, whilst it is highest for temperature (Hawkins and Sutton 2009). Moreover, the uncertainty of precipitation in the CMIP3 models for the 21st century is very large and different models even disagree on sign of change in trends (Biasutti et al. 2008). The precipitation will increase (decrease) in some (other) regions at the end of 21st century, whilst temperature will increase almost everywhere, though magnitude of increase/decrease varies from place to place and model to model (Meehl et al. 2005; Almazroui et al. 2016).

The decision-makers and stakeholders in the Arabian Peninsula are looking for reasonable climate projections for their adaptation and strategic planning. Since there are large uncertainties in climate projections, an alternative to reducing the spread could be useful to develop adaptation strategies for most extreme ensemble members (e.g., Daron et al. 2014; Whetton et al. 2012; Hallegatte 2009). Since there is no common sense what the best strategy is, the filtering out of well performing models for climatic parameters (such as precipitation and temperature) could be beneficial for climate change impact studies over the Arabian Peninsula. The main objectives of this study are (1) categorization of the CMIP3 models into different groups based on their individual performance in simulation of present day climate over the Arabian Peninsula and (2) assessment of uncertainties in the simulated potential future climate over the Arabian Peninsula by the different categories of CMIP3 models.

In a recent study, Almazroui et al. (2016) examined the future changes in temperature and precipitation over the Arabian Peninsula using CMIP3 models without considering the performance of individual CMIP3 models in the present day climate. There is no comprehensive study over the Arabian Peninsula that assesses the uncertainties in the future climate projections for different categories of CMIP3 models. The present study fills this gap by first analyzing the CMIP3 data sets and categorizing the models into different groups based on their performance in the present day climate. Since the IPCC has also released its latest fifth phase of CMIP data (CMIP5) through its Fifth Assessment Report (AR5), in a subsequent study, an assessment of potential future climate and associated uncertainties over the Arabian Peninsula based on CMIP5 data set is documented.

The paper is organized as follows. Section 2 describes the data and methodology used in this paper. Section 3 presents the main results of this study. Summary and conclusions are given in the Sect. 4.

2 Data and methodology

2.1 Data and models

In the present study, the data from available 22 CMIP3 models from the CMIP archives (<http://www-pcmdi.llnl.gov/>) are analyzed. Table 1 shows a list of models used in this study. First, we examined the performance of the CMIP3 models over the Arabian Peninsula for the present climate (1970–1999). For this purpose, we first employed the observational data for surface air temperature and precipitation from 27 stations across Saudi Arabia which covers about 80% area of the Peninsula. To compare CMIP3 model data with station observation, we extracted data from the grid point where stations are located. The model data are grid averaged values, whereas station data represent point values and this may also introduce some additional uncertainty in the results. However, this is the most common technique used to compare the model data with station observations (Islam 2009; Islam et al. 2008; Islam and Uyeda 2007). To avoid this uncertainty, we also assessed the performance of CMIP3 models using gridded ($1^\circ \times 1^\circ$ grid) CRU observational data set obtained from the Climatic Research Unit (CRU TS 3.23, Mitchell and Jones 2005; New et al. 2000).

2.2 Methodology

Prior to analyzing the CMIP3 model outputs with different horizontal resolutions (see Table 1), all 22 CMIP3 model data sets are regridded to a common $1^\circ \times 1^\circ$ grid. In the

Table 1 CMIP3 models used in this study. The references for these models are available in Almazroui et al. (2016)

	IPCC ID of the model	Country	B1	A1B	A2	Atmospheric resolution (lat × lon)
a	BCC-CM1	China			*	1.9° × 1.9°
b	BCCR-BCM2.0	Norway	*		*	1.9° × 1.9°
c	CCCMA-CGCM3.1(T47) ^{P,S}	Canada	*	*	*	2.8° × 2.8°
d	CNRM-CM3	France	*	*	*	1.9° × 1.9°
e	CSIRO-Mk3.0 ^{P,S}	Australia	*	*	*	1.9° × 1.9°
f	GFDL-CM2.0	USA	*	*	*	2.0° × 2.5°
g	GFDL-CM2.1 ^{P,S}	USA		*	*	2.0° × 2.5°
h	GISS-AOM ^{T,S}	USA	*	*		3° × 4°
i	GISS-EH	USA		*		4° × 5°
j	GISS-ER	USA	*		*	4° × 5°
k	IAP-FGOALS-g1.0	China	*	*		2.8° × 2.8°
l	INM-CM3.0	Russia	*	*	*	4° × 5°
m	IPSL-CM4	France	*	*	*	2.5° × 3.75°
n	MIROC3.2(hires) ^{T,S}	Japan	*	*		1.1° × 1.1°
o	MIROC3.2(medres) ^{T,S}	Japan	*	*	*	2.8° × 2.8°
p	MIUB-ECHO-G ^{T,S}	Germany/Korea	*	*	*	3.9° × 3.9°
q	ECHAM5/MPI-OM ^{T,S}	Germany	*	*	*	1.9° × 1.9°
r	MRI-CGCM2.3.2 ^{T,S}	Japan	*	*	*	2.8° × 2.8°
s	NCAR-CCSM3	USA	*	*	*	1.4° × 1.4°
t	NCAR-PCM	USA	*	*	*	2.8° × 2.8°
u	UKMO-HadCM3 ^{P,T,S}	UK	*	*	*	2.5° × 3.75°
v	UKMO-HadGM ^{P,S}	UK		*		1.3° × 1.9°

The superscripts P, T, and S represent the precipitation-based, temperature-based, and selected best performing models, respectively (see text for more information). The ‘*’ in the fourth, fifth, and sixth columns shows the model run available and used for future analysis of B1, A1B, and A2 scenarios

next step, the temperature and precipitation biases for individual models as well as for multi-model ensemble (MME) are calculated with reference to the observations for the present climate (1970–1999). Note that the MME is calculated with equal weight. Only grid points covering the land areas are taken into consideration for this analysis.

Based on simulated temperature and precipitation biases, standard deviation, annual cycle, systematic error (SyE), the normalized root-mean-square error (NRMSE), the standard error (SE), and the CMIP3 models are categorized into four different categories, namely (1) all 22 CMIP3 models, (2) precipitation-based models, (3) temperature-based models, and (4) best performing models. The models which simulated the domain averaged precipitation (temperature) bias between ± 1 intermodel standard deviation are referred to as precipitation (temperature)-based models. The precipitation (temperature)-based models are further assessed in obtaining the annual cycle, SyE, NRMSE, and SE measures compared to the observations. Only those CMIP3 models which simulated low SyE, NRMSE, and SE together with annual precipitation (temperature) cycle that closely resembles to observations

are kept into the above categories. The fourth category of the models is named as the best performing models. This category includes CMIP3 models having both precipitation and temperature biases within ± 1 intermodel standard deviation. In addition, the best performing models simulated the annual cycles of temperature and precipitation that closely resembles to the observations and display small values of SyE, NRMSE, and SE compared to the other three categories (see Sect. 3 for further details).

In the next step, the changes in temperature and precipitation in the future climate and associated uncertainties are computed for the mid (2021–2050) and end (2070–2099) of the 21st century relative to the present climatology (1970–1999) for both all (22 CMIP3) and best performing models. The future projections are examined for the Special Report on Emission Scenarios (SRES) B1, A1B, and A2 (IPCC 2000). To quantify the uncertainties associated with projected temperature and precipitation over the Arabian Peninsula, we used ± 1 intermodel standard deviation (STD) and the intermodel range between the minimum and maximum value as metrics for both the all and best performing models. We assessed the robustness of

the future climate change for both categories of model ensembles. Following the previous studies (e.g., Almazroui et al. 2016; Heansler et al. 2013a, b; Solomon et al. 2007), we also employed a measure which describes the agreement of the different model projections in the direction of change. An increase (or decrease) in the projected signal is considered to be robust if at least 66% of the models agree in the direction of change. We used the Mann–Kendall trend test (Kendall 1976) to assess the significance of the trends in the temperature and precipitation over the Arabian Peninsula in the 21st century. In addition to above, we also examined the temperature projection for the future period by adding the present day bias to the projected temperatures. This is referred as the corrected temperature. Although, it is not necessary that the bias in the present climate continues in the future, but the bias corrected future values of the parameters may provide some reasonable estimates for long-term future planning.

3 Results and discussion

3.1 Analysis of present day climate (1970–1999) climate

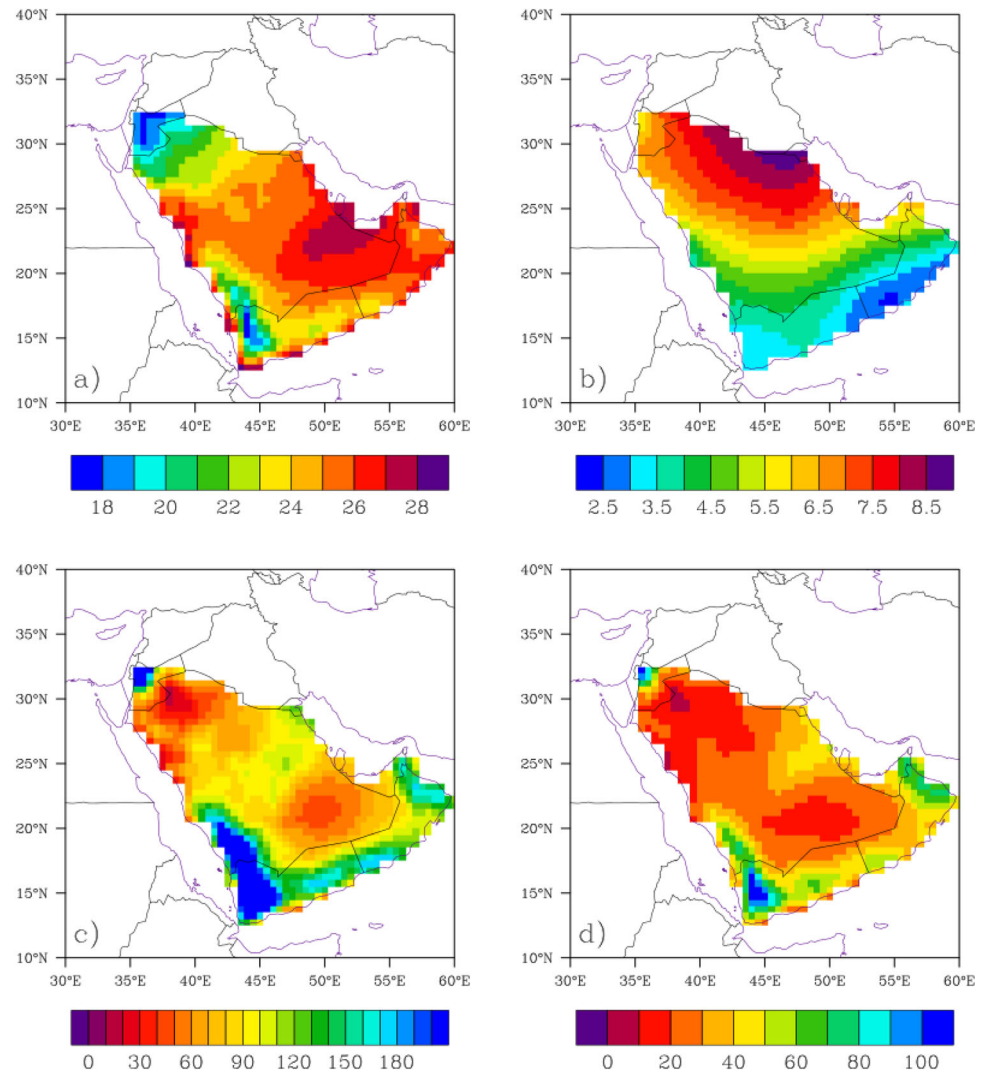
Prior to the analysis of CMIP3 database, a brief description on the study area is important to understand the climatic conditions over the Arabian Peninsula. The Arabian Peninsula (comprising of Bahrain, Kuwait, Oman, Qatar, Saudi Arabia, United Arab Emirates, and Yemen) is located in the southwest Asia, which is actually the junction of Asia and Africa. The world's largest continuous sand desert the Rub Al-Khali is located in Saudi Arabia, a unique country that covers about 80% area of the Arabian Peninsula (Almazroui et al. 2012a). The peninsula is surrounded by the water bodies such as the Red Sea (in the West), Arabian Gulf (in the East), and the Arabian Sea (in the South). Its climate is influenced by the Mediterranean Sea region in the winter season and by the South Asian Summer Monsoon in the summer season. The Sudan low also influences the climate of the peninsula. The southern part of the Arabian Peninsula (Saudi Arabia to western Yemen) is covered by the mountains with maximum elevation about 2200 m (Almazroui 2011). The mountain ranges have sharp elevation to the west near the Red Sea and they gradually decrease towards the East. The western sharp edge of the mountain facing the Red Sea plays an important role in the occurrence of heavy rainfall in the peninsula (Chakraborty et al. 2006). In general, the climate of the peninsula is characterized by arid and semi-arid (Almazroui et al. 2012b). The middle-to-north of Saudi Arabia is dry (below 150 mm), while the southwest of the peninsula is wettest (above 150 mm). The annual total

precipitation varies from 25 mm (at a station Wejh, 26.20°N and 36.47°E) to 230 mm (at a station Abha, 18.23°N and 42.66°E), and is markedly influenced by seasonal variations (Almazroui et al. 2012a, b). The low temperature (below 21 °C) persists in the northwest and southwest of the peninsula while relatively high temperature (24–27 °C) in the middle-to-south. In the present day climate, the observed data show a significant decreasing trend (47.8 mm/decade) in the precipitation, while the mean temperature over the Arabian Peninsula significantly increased by 0.60 °C/decade (Almazroui et al. 2012a).

The annual mean temperature and precipitation and their standard deviation over the Arabian Peninsula for present day climate show that the eastern and central-western parts of the peninsula have the highest annual mean temperature (Fig. 1). On the other hand, the northwestern and south-western mountainous regions receive slightly low temperature compared to the eastern and central-western parts. The temperature standard deviation is larger in the northern parts of the Arabian Peninsula compared to the southern and southeastern parts. The large variability in the annual mean temperature over northern parts of the Arabian Peninsula is generally associated with the eastward moving synoptic systems from the Mediterranean region throughout the year, particularly in the winter season that influence largely the near surface temperature over this region. The larger parts of the Arabian Peninsula, particularly the northwestern and over the sand desert Rub Al-Khali (Almazroui et al. 2012a, b), observe dry weather throughout the year. Precipitation is highly variable and the south-western mountainous region of Saudi Arabia and Yemen receive the highest annual mean precipitation which mainly occurs in the summer season (Fig. 1c, d). In addition to the above the eastern parts of Yemen, Oman and the western parts of Jordan also receive enhanced annual mean precipitation. The precipitation over Yemen/Oman occurs in the summer months, whilst over Jordan, it is from the winter months. The standard deviation of precipitation is also large over these regions. Almazroui et al. (2012b) showed that a large proportion of the annual mean precipitation over the Arabian Peninsula is received during the wet season (November–March). Due to its geographical location, the larger contribution to the annual mean rainfall comes from extreme precipitation events that occur in a short interval of time (Almazroui et al. 2012a, b).

As mentioned earlier, Almazroui et al. (2013) analyzed precipitation from 22 IPCC AR4 multi-model data sets for the period (1979–2000) and found two groups of models (each composed of 5 models) performing better over the Arabian Peninsula in different seasons. In the present study, we further examined the performance of individual CMIP3 models over the Arabian Peninsula for both temperature and precipitation, and categorized them into four

Fig. 1 **a** Mean temperature and **b** standard deviation, based on CRU observations for the period 1970–1999. **c–d** same as **a**, **b** except for precipitation. The unit of temperature is °C and precipitation is mm/year



categories (discussed earlier). The spatial distribution of temperature and precipitation biases by all models with respect to the CRU observations over the Arabian Peninsula is shown in Figs. 2 and 3. It can be seen that the spatial bias in the temperature and precipitation varies widely among the CMIP3 models. Most of the CMIP3 models simulate warm (cold) bias over the southern (central and northern) parts of the peninsula. The intermodel range for temperature bias between the all models varies within $>\pm 7^\circ\text{C}$ over the Arabian Peninsula (Fig. 2). The MME mean shows a reduction of cold (warm) bias over the central and northwestern (southern and eastern) parts of the peninsula. Similar to the temperature, the spatial pattern of the precipitation bias also varies among the CMIP3 models. The larger portion of the Arabian Peninsula is dominated by the dry bias in most of the models simulations. However, some CMIP3 models (Fig. 3b, d, k, n, o, p, s, t; Table 1) also display wet bias specially over the southeastern parts of the peninsula. Interestingly, the MME

reduces remarkably the wet bias over the southern and southeastern parts of the Arabian Peninsula.

From the above analysis, it is difficult to assess which of the CMIP3 models perform better in simulation of the temperature and precipitation over the Arabian Peninsula. We further examined the domain averaged temperature and precipitation biases over the peninsula using both CRU data and surface observations (Fig. 4). For brevity, the results with CRU data are not shown here. It can be seen that the models performing better for temperature are not necessarily well suited for precipitation (Fig. 4a, c). Furthermore, the variability in the temperature and precipitation bias also varies largely among different models. Based on the above analysis (Figs. 2, 3, 4), the CMIP3 models are grouped into four categories. The first category, all, includes all 22 CMIP3 models irrespective of their performance over the Arabian Peninsula.

The second category of models named as temperature-based models. The temperature bias simulated by these

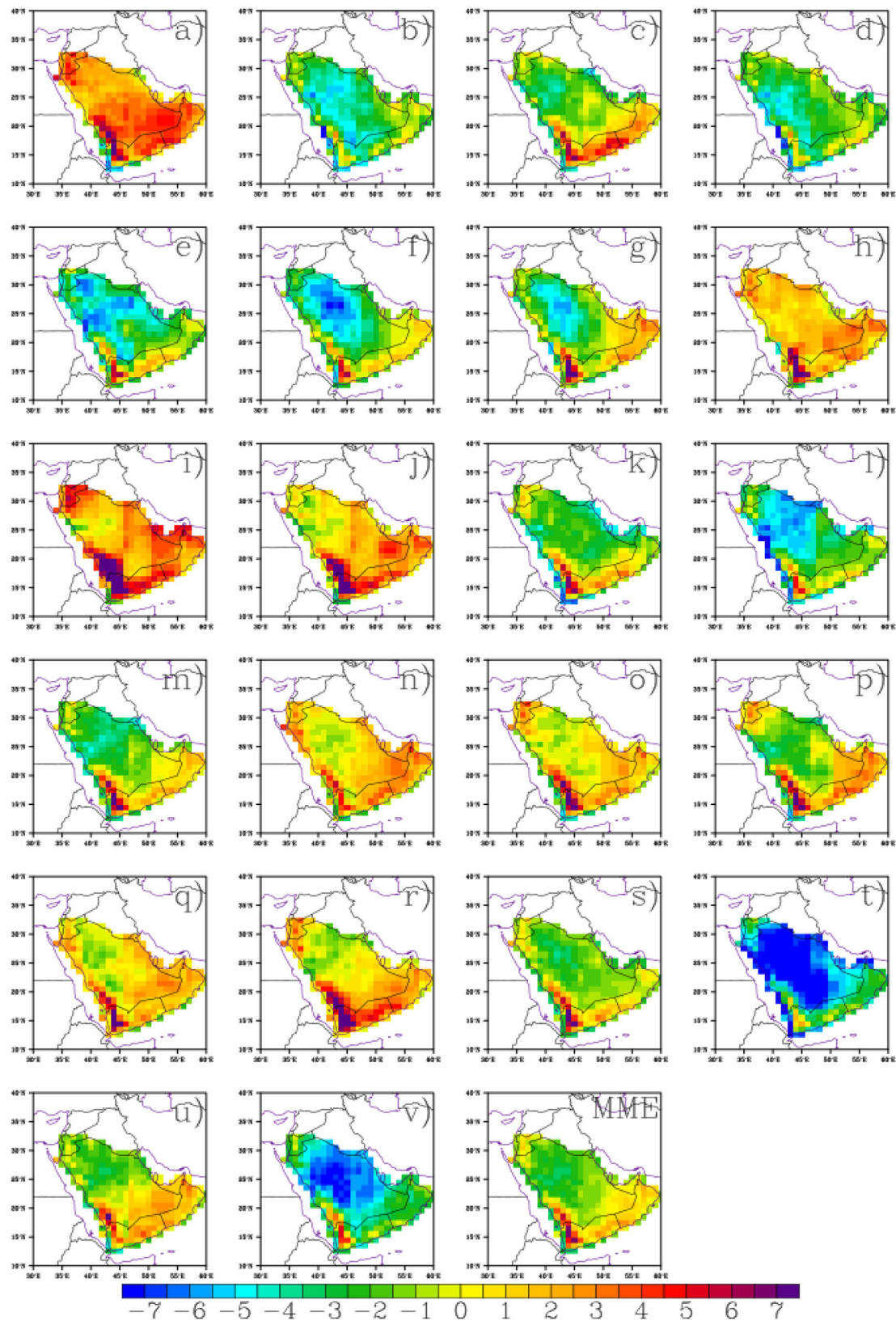


Fig. 2 Simulated mean temperature bias (in °C) over the Arabian Peninsula by 22 CMIP3 models listed in Table 1. The bias is computed with reference to the CRU observational data set for the

present climate (1970–1999). The labels on the upper right corner in each panel correspond to the models listed in Table 1. The last panel shows the multi-model ensemble (MME) mean

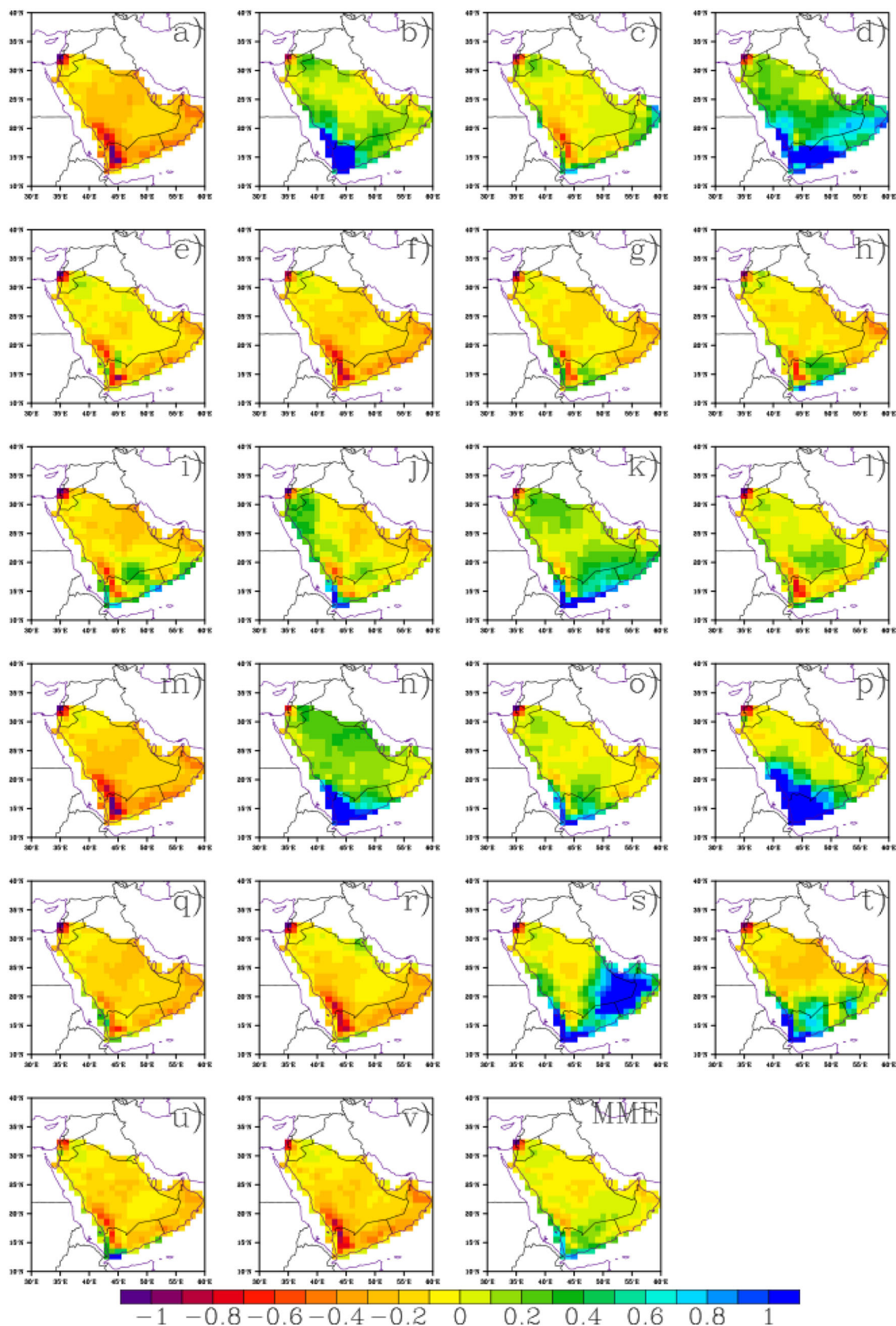


Fig. 3 Same as Fig. 2 except for precipitation (mm/month)

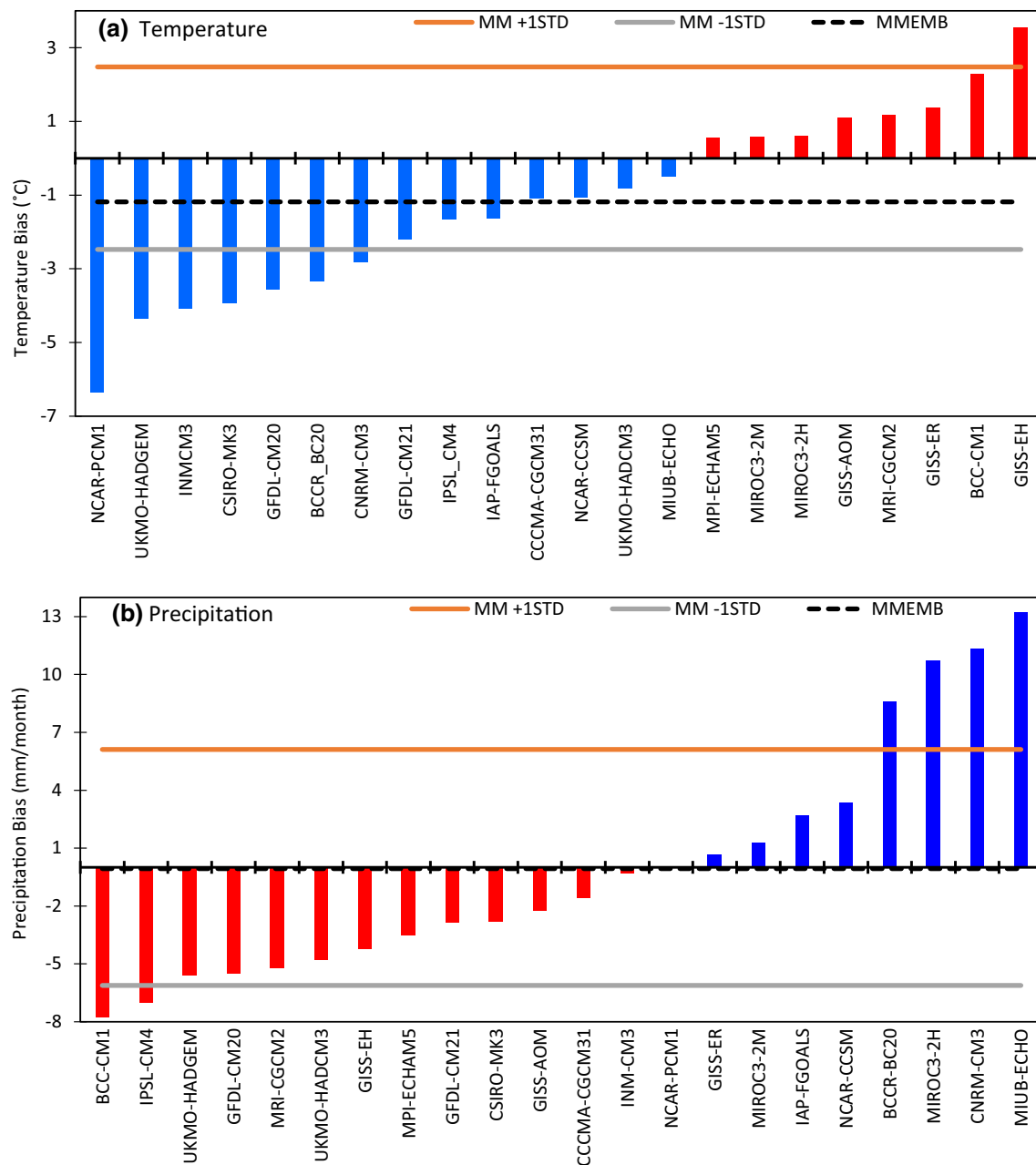


Fig. 4 Mean bias of the CMIP3 models (listed in Table 1) with respect to the station observation **a** temperature (unit: °C) and **b** precipitation (unit: mm/month). The CMIP3 models data are extracted at observation coordinates and averaged over 27 locations.

models domain lies within ± 1 intermodel standard deviation. These models simulated lowest SysE, NRMSE, and SE with reference to observed surface air temperature (Table 2). Results show that temperature values estimated by most of the CMIP3 models follow the annual cycle except BCC-CM1 (Fig. 5). In addition, we also applied pattern matching technique for the annual cycle to examine the performance of CMIP3 models over the Arabian Peninsula. The monthly temperature simulated by

The colored lines (orange/grey) show multi-model ± 1 standard deviation. The multi-model ensemble mean bias (MMEMB) is shown by the dashed line. The red (blue) colors are adopted to indicate the warm (dry) and cold (wet) CMIP3 models over the Arabian Peninsula

temperature-based models closely following the pattern of the observations. It is found that 7 models out of 22 follow temperature trends that are closer to the observations. These models are referred as temperature-based models and are shown with superscript T in Table 1.

The third category of models is referred as precipitation-based models. These are the models which display the precipitation bias within ± 1 intermodel standard deviation. In addition to low precipitation bias, the third category of

Table 2 CMIP3 models simulated systematic error (SyE), normalized root-mean-square error (NRMSE), and standard error (SE) with reference to the observed temperature

Models	SyE	NRMSE	SE
BCCR-BCM2	-3.72	0.15	0.60
BCC-CM1	1.86	0.08	2.13
CCCMA-CGCM31	-1.61	0.07	0.63
CNRM-CM3	-3.13	0.13	1.10
CSIRO-Mk3	-4.50	0.18	1.02
MPI-ECHAM5	0.28	0.01	0.60
GFDL-CM20	-4.01	0.16	0.83
GFDL-CM21	-2.60	0.11	1.00
GISS-AOM	0.71	0.03	0.71
GISS-EH	3.18	0.13	0.69
GISS-ER	0.96	0.04	0.72
UKMO-HadCM3	-1.22	0.05	0.64
UKMO-HadGEM	-4.84	0.20	0.97
IPSL-CM4	-2.10	0.09	0.60
IAP-FGOALS	-1.98	0.08	0.70
INM-CM3	-4.47	0.18	0.53
MIROC3-2H	0.24	0.01	0.69
MIUB-ECHO	-0.79	0.03	0.44
MIROC3-2M	0.25	0.01	0.56
MRI-CGCM2	0.75	0.03	0.41
NCAR-CCSM3	-1.42	0.06	0.56
NCAR-PCM	-6.74	0.27	0.52
Average	-1.59	0.09	0.76

models also reveals lowest SysE, NRMSE, and SE with reference to observed precipitation (Table 3). The annual cycle of the simulated precipitation reveals that most of the CMIP3 models overestimate the rainfall during the dry (June to September) season, while they underestimate rainfall during the wet season (November–April) (Fig. 6). Simulations of precipitation annual cycle reveals that only few models are closer to the observations (Fig. 6). By applying the pattern matching technique and a careful examination of simulated precipitation biases and errors analysis reveals that only five models out of 22 are suitable for precipitation analysis over the Arabian Peninsula. This group of model is referred to as precipitation-based model and is represented by superscript P in Table 1. The fourth category of the CMIP3 models is named as the best performing models. These are the models which display lowest precipitation and temperature bias over the Arabian Peninsula. The best performing models are filtered out from second and third categories based on their individual performance in simulations of temperature and precipitation biases as well as the annual cycle, SyE, NRMSE, SE,

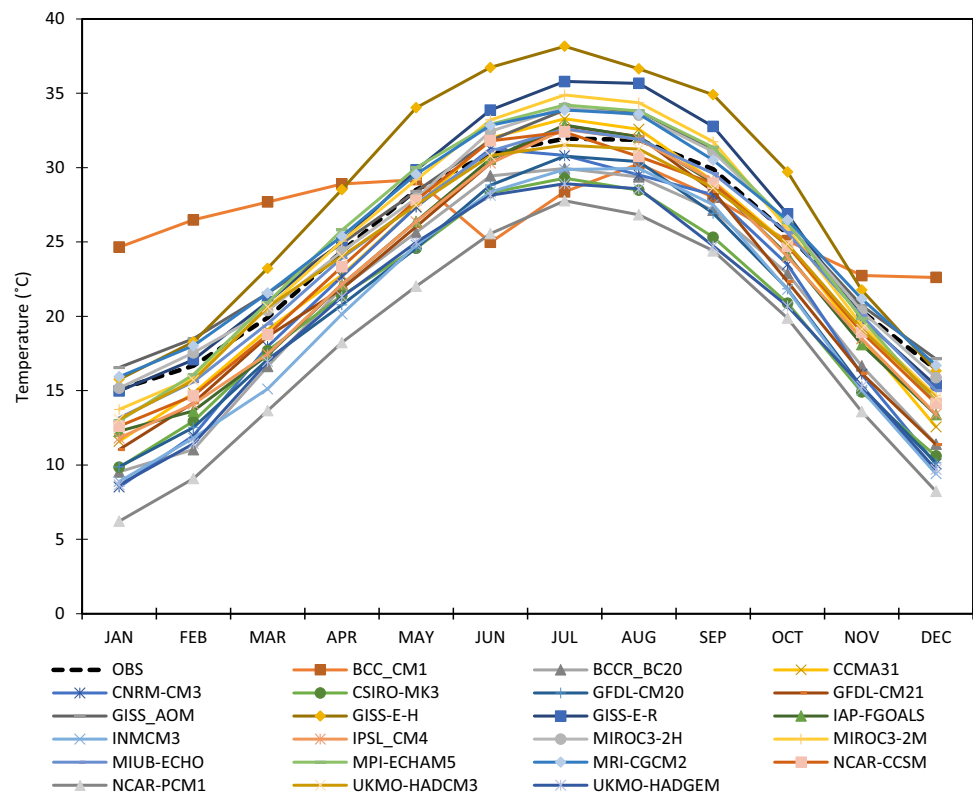
etc. (Tables 2, 3) over the peninsula. Based on the above analysis, the changes in future signals of temperature and precipitation and associated uncertainty are analyzed only for all and best performing models.

3.2 Changes in temperature and precipitation in the future climate

In a recent study, Almazroui et al. (2016) examined the future climate change over the Arabian Peninsula using CMIP3 models without taking into account performance of the *individual* CMIP3 models in simulation of present day climate. Our results for the first category (i.e., all models) are almost similar to those presented by Almazroui et al. (2016) in their Figs. 2 and 5; however, the future climate projections are more pronounced in case of best performing models presented in this study. Figure 7 shows the future changes in temperature over the Arabian Peninsula for three SRES scenarios B1, A1B, and A2. In all cases, the central and northern parts of the Arabian Peninsula display enhanced change in future temperature compared to its surroundings. Projected temperature values over the Arabian Peninsula for three future scenarios B1, A1B, and A2 ranges between ~ 1 and ~ 2.9 °C for near future (2021–2050) and ~ 1.8 to ~ 4.2 °C for far future (2070–2099) (Fig. 7). Furthermore, it can be seen that the more than 66% of the models temperature in the CMIP3 projections agree in sign of future changes (shown by the dotted areas). Compared to the all models, the best performing models also project similar spatial pattern of future changes in temperature (Fig. 8). However, as mentioned earlier, the future changes in the temperature are more pronounced in case of best performing models compared to the all models. Similar to the all models ensemble, the best performing models also display higher temperature changes in the central and northern parts of the peninsula. For the best performing models, the projected temperature values for three future scenarios B1, A1B, and A2 range from 0.96 to ~ 2.2 °C for near future (2021–2050) and ~ 1.9 to ~ 5.2 °C for far future (2070–2099) (Fig. 8), which is slightly larger than the all models.

The projected changes in annual mean precipitation over the Arabian Peninsula show a southeast–northwest dipole like pattern with enhanced (reduced) precipitation over the southeastern (northwestern) parts of the peninsula (Fig. 9). This pattern is almost similar to that shown by Almazroui et al. (2016) in their Fig. 5, though a time slot for the two studies is slightly different. The projected change in annual precipitation over the Arabian Peninsula ranges to $\pm 20\%$ for the near future (2021–2050) and nearly $\pm 50\%$ for the far future (2070–2099). Similar to future temperature changes, the future precipitation change signals are more intense towards the end of the 21st century. The dotted

Fig. 5 Annual cycle of temperature (unit: °C) obtained from all 22 CMIP3 models and compared with station observations averaged over the period 1970–1999. The CMIP3 models' data are extracted at nearest grid point of observation coordinate and averaged over 27 locations. The observation is shown by *black dashed line*



areas in Fig. 9 show the regions where at least 66% of the CMIP3 models agree in the sign of direction.

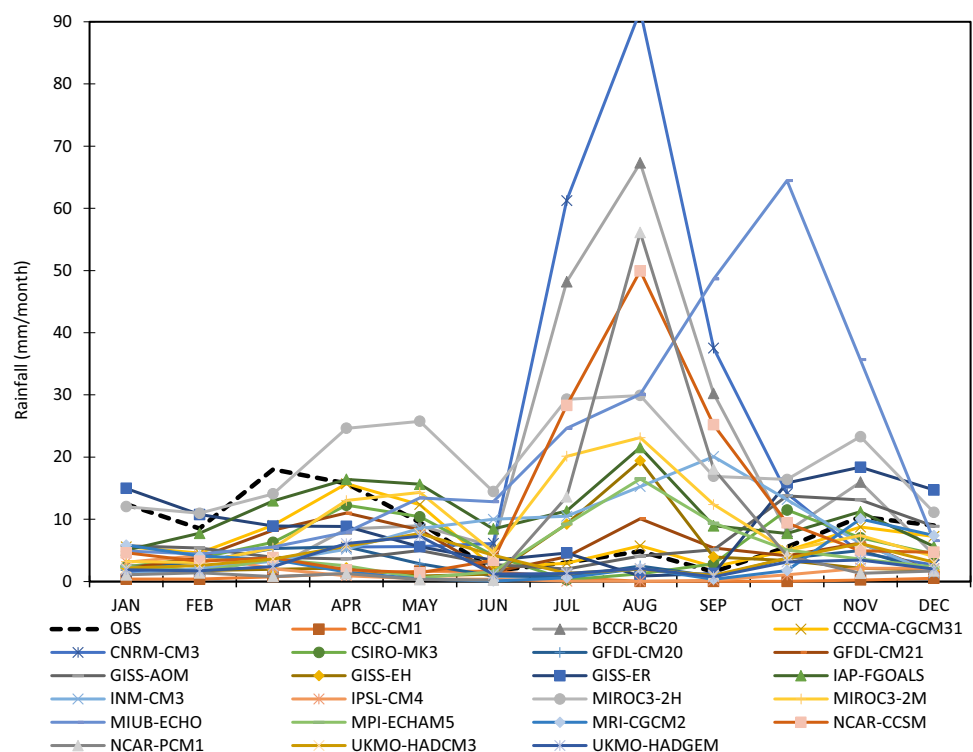
For best performing models, the MME change also show nearly similar dipole like pattern as shown for the all models ensemble (Fig. 10). However, the future increase in precipitation is more pronounced over the southern parts of Saudi Arabia, United Arab Emirates, and Yemen (e.g., Fig. 10e, f) compared to the all models ensemble which shows a future intensification over eastern parts of Saudi Arabia and adjacent countries of United Arab Emirates and Oman (e.g. Fig. 9e, f). Moreover, the reduction in the future precipitation is also more pronounced in the best performing models over the northwestern parts of Saudi Arabia compared to the all models. Similar to the temperature changes, for the best performing models, the future changes of annual mean precipitation signals are more intense towards the end of the 21st century. Due to its geographical location, the Arabian Peninsula receives very low amount of annual mean precipitation. The main contribution of this annual mean precipitation comes from a few heavy rainfall events (Almazroui et al. 2014). It is not clear from this analysis whether extreme rainfall events will increase over this region in the future climate. Furthermore, to what extent the best performing global model simulations reproduce the observed precipitation extremes over this region. These questions are open for further studies.

3.3 Uncertainty in projections of temperature and precipitation

Figure 11 shows the evolution of the annual mean temperature anomalies from 2001 to 2100 averaged over the Arabian Peninsula. The MME mean with ± 1 intermodel standard deviation (STD) and intermodel range is also shown for all (Fig. 11a, c) and best performing (Fig. 11b, d) models. It can be seen that the temperature increases continuously from the 2001 to the end of the 21st century under the B1, A1B, and A2 scenarios, with the strongest warming under A2 at the end of this century. The projected difference in the temperature values among the three scenarios is weak in the early 21st century, and gradually increases with integration of time. The B1 scenario shows lower temperature changes during the all integration period; however, A1B displays slightly higher values compared to B1 till the end of 21st century. After 2070s, the temperature values for A2 are higher compared to both B1 and A1B. It is important to note that the ± 1 intermodel STD and intermodel range also show larger spread in case of all models (Fig. 11a, c) compared to the best performing models (Fig. 11b, d). Furthermore, the MME projection of temperature under A1B and A2 scenarios are slightly higher towards the end of 21st century for best performing models compared to the all models (Fig. 11a, b). Based on Mann–Kendall trend test, the increasing trends of future

Table 3 CMIP3 models simulated systematic error (SyE), normalized root-mean-square error (NRMSE), and standard error (SE) with reference to the observed precipitation

Models	SyE	NRMSE	SE
BCCR-BCM2	8.58	1.02	18.96
BCC-CM1	-7.85	0.93	0.54
CCCMA-CGCM3	-1.14	0.13	2.77
CNRM-CM3	11.14	1.32	25.61
CSIRO-Mk3	-2.15	0.26	4.42
MPI-ECHAM5	-3.46	0.41	4.61
GFDL-CM20	-5.59	0.66	1.04
GFDL-CM21	-3.18	0.38	3.33
GISS-AOM	-2.27	0.27	4.06
GISS-EH	-4.29	0.51	5.49
GISS-ER	0.79	0.09	5.74
UKMO-HadCM3	-4.42	0.52	2.09
UKMO-HadGEM	-5.69	0.67	1.70
IPSL-CM4	-7.05	0.83	1.23
IAP-FGOALS	2.61	0.31	5.11
INM-CM3	-0.58	0.07	3.96
MIROC3-2H	10.49	1.24	7.14
MIUB-ECHO	12.81	1.52	17.42
MIROC3-2M	1.45	0.17	7.04
MRI-CGCM2	-5.34	0.63	2.85
NCAR-CCSM3	3.55	0.42	13.30
NCAR-PCM	-0.28	0.03	14.90
Average	-0.09	0.56	6.97

Fig. 6 Annual cycle of monthly rainfall (unit: mm) obtained from all 22 CMIP3 models and compared with observations averaged over 1970–1999. The CMIP3 rainfalls are extracted at nearest grid point of observation coordinate and averaged over 27 locations. The observation is shown by *black dashed line*

change in temperature for all/best models towards the end of twenty-first century are significant to 99% level for all three scenarios A2, A1B, and B1.

To further analyze the uncertainties in temperature projection, the Box-and-Whisker plot in Fig. 12 shows MME mean temperature with ± 1 intermodel STD and intermodel range for near future (2021–2050) and far future (2070–2099) periods. The results show an increase in uncertainty with time under the three emissions scenarios (Fig. 12a, b). By the end of the 21st century, the annual mean temperature is projected to increase by 2.32 ± 2.45 , 3.49 ± 2.49 , and 3.82 ± 1.47 °C, relative to the present day climate, under the B1, A1B, and A2 scenarios, respectively, while the intermodel ranges are projected to be -3.36 to 6.08 , -2.26 to 7.68 , and -1.79 to 7.40 °C, respectively (Fig. 12a, b).

The uncertainties associated with temperature projection decrease remarkably for best performing models compared to the all models (Fig. 12a, b). The results further show an increase in the MME mean temperature for best performing models but a decrease in uncertainty range under the three emissions scenarios. By the end of the 21st century, the annual mean temperature is noted to be increased by 3.85 ± 1.54 , 4.91 ± 1.61 , and 5.36 ± 1.47 °C, relative to the present climate, under the B1, A1B, and A2 scenarios, respectively, while the intermodel ranges are projected to be 0.84 to 5.96 , 1.94 to 7.29 , and 2.75 to 7.10 °C, respectively (Fig. 12c, d).

Fig. 7 Future changes in all (22 CMIP3) multi-model ensemble mean temperature (unit: °C) for near future (2021–2050, *left panel*) and far future (2070–2099, *right panel*) with reference to the present climate (1970–1999). *Dotted areas* indicate regions where at least 66% of CMIP3 models agree on sign of future changes signals of temperature over the Arabian Peninsula. The SRES scenarios are B1 (*top*), A1B (*middle*), and A2 (*bottom*)

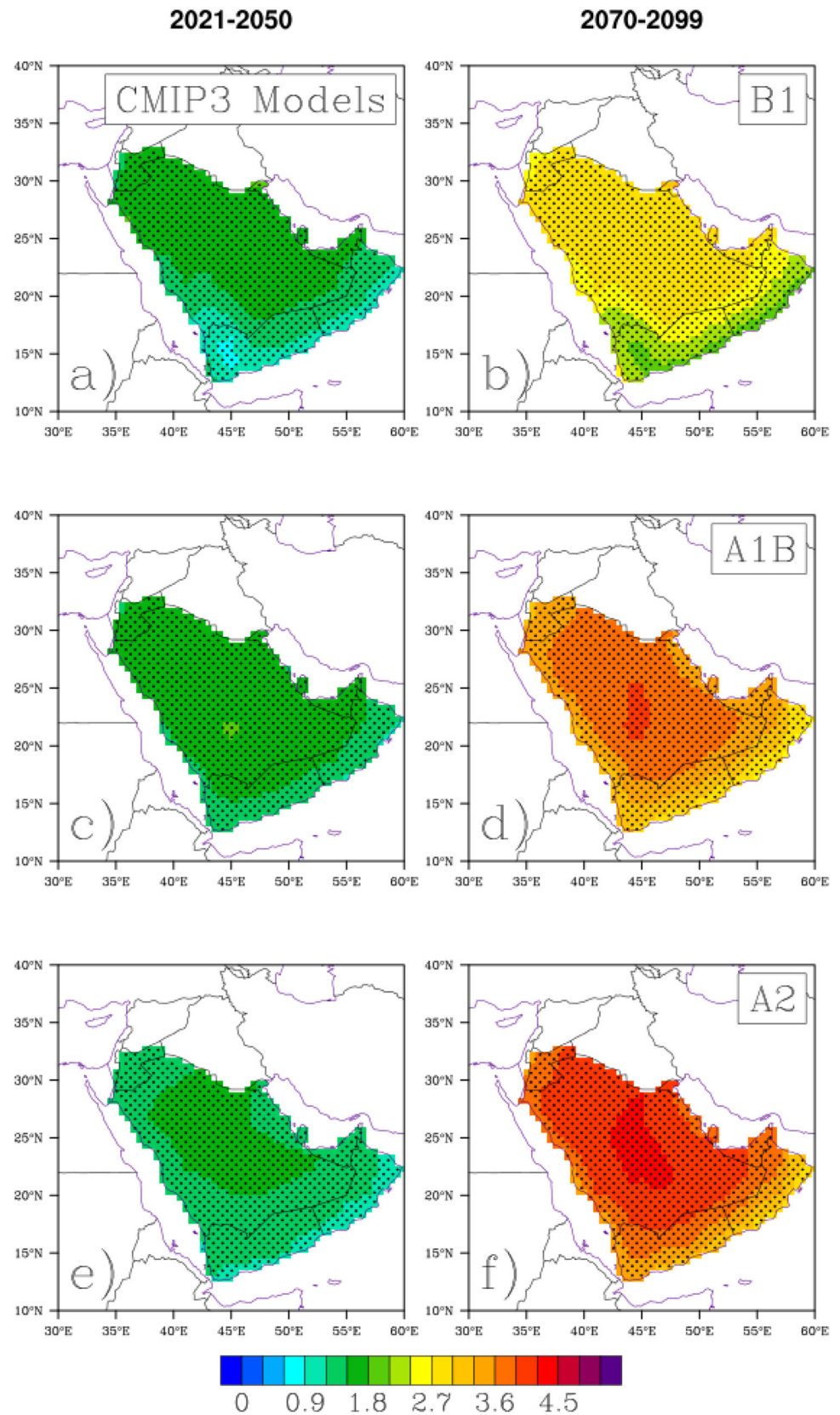


Fig. 8 Same as Fig. 7 except for the selected best performing models

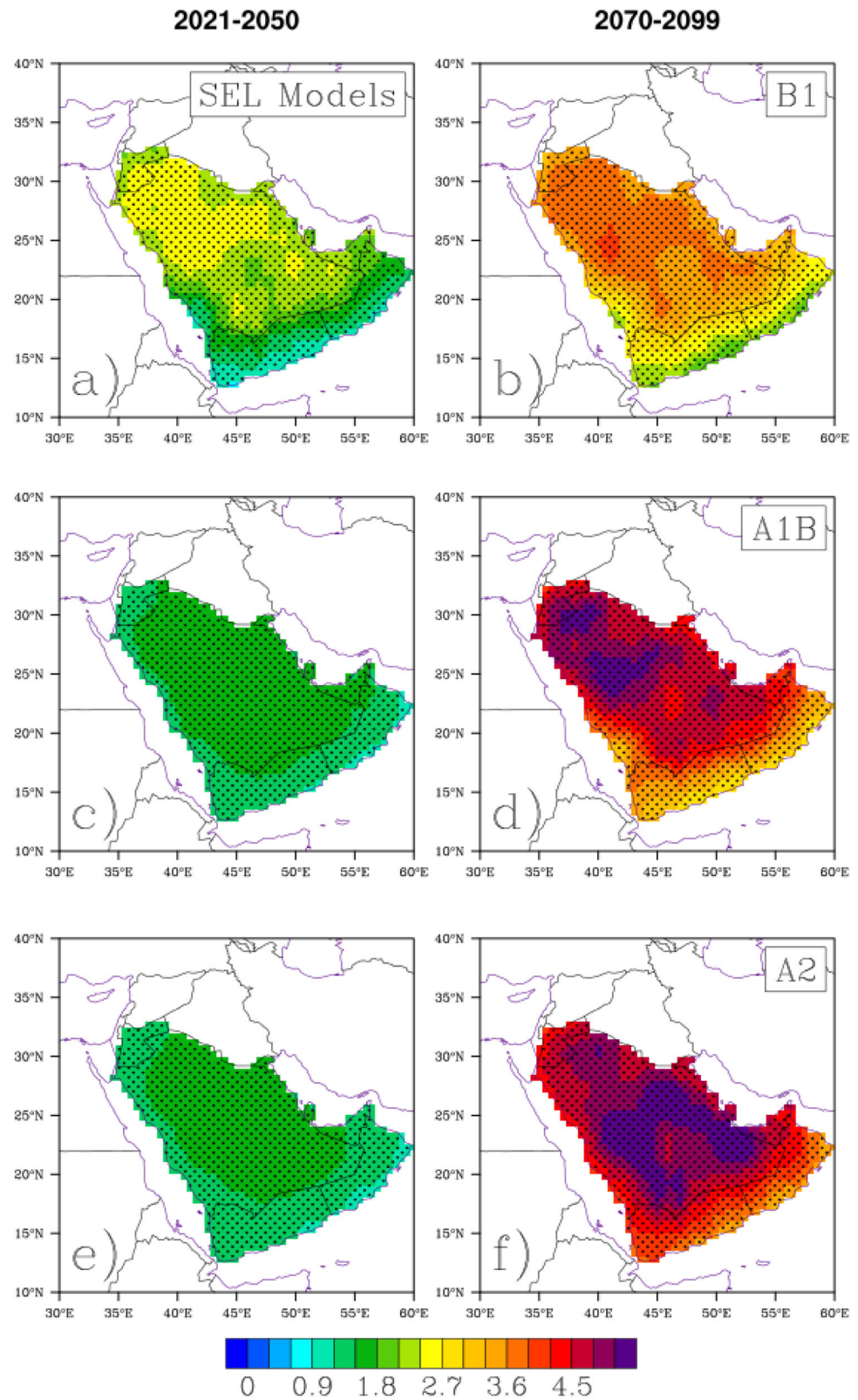
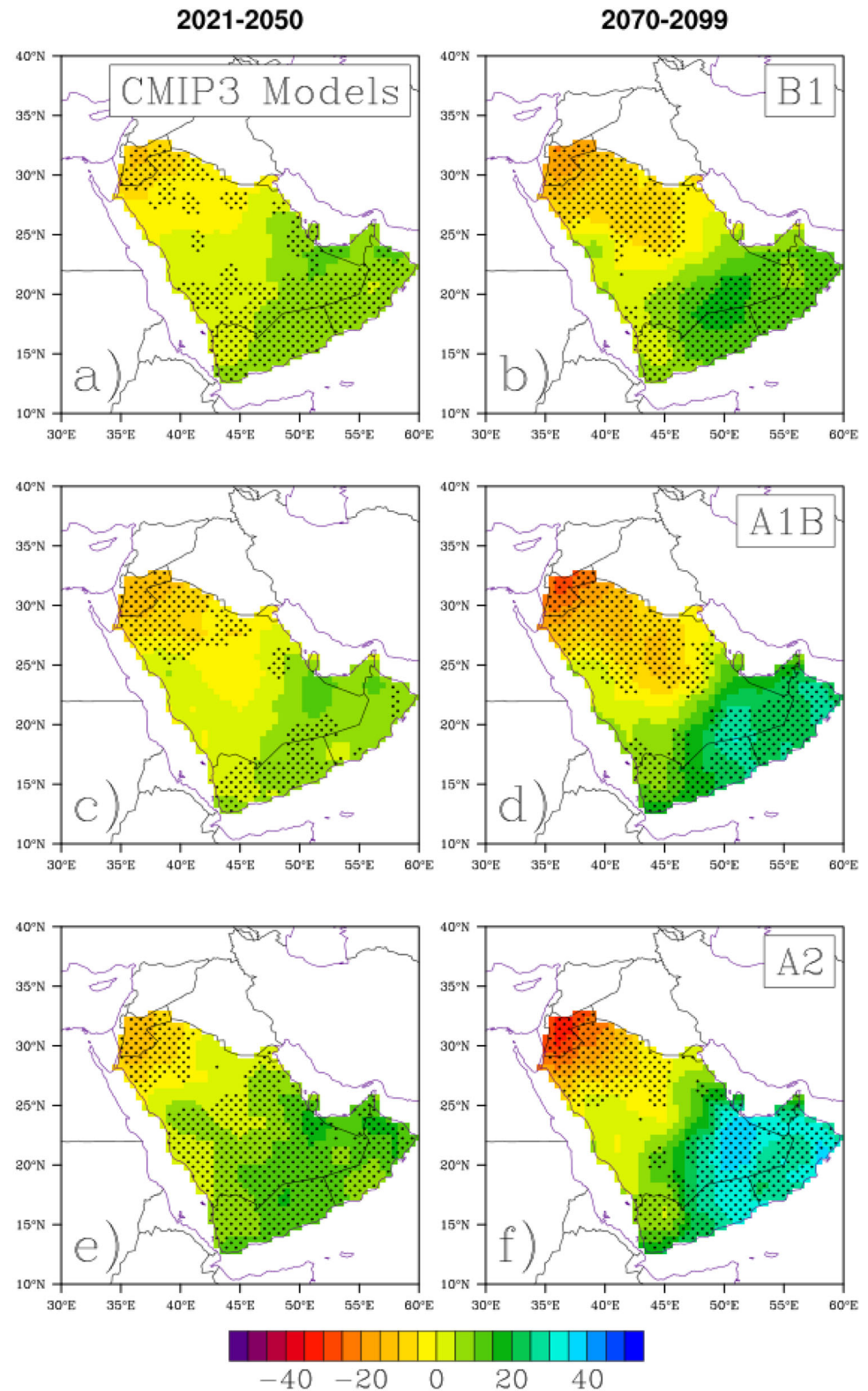


Figure 13 shows the evolution of the annual mean precipitation anomaly (in %) from 2001 to 2100 averaged over the Arabian Peninsula. The MME (solid lines) with ± 1

intermodel STD and intermodel range (color shading in Fig. 13a, b) is also shown for all and best performing models. Unlike temperature, the domain averaged

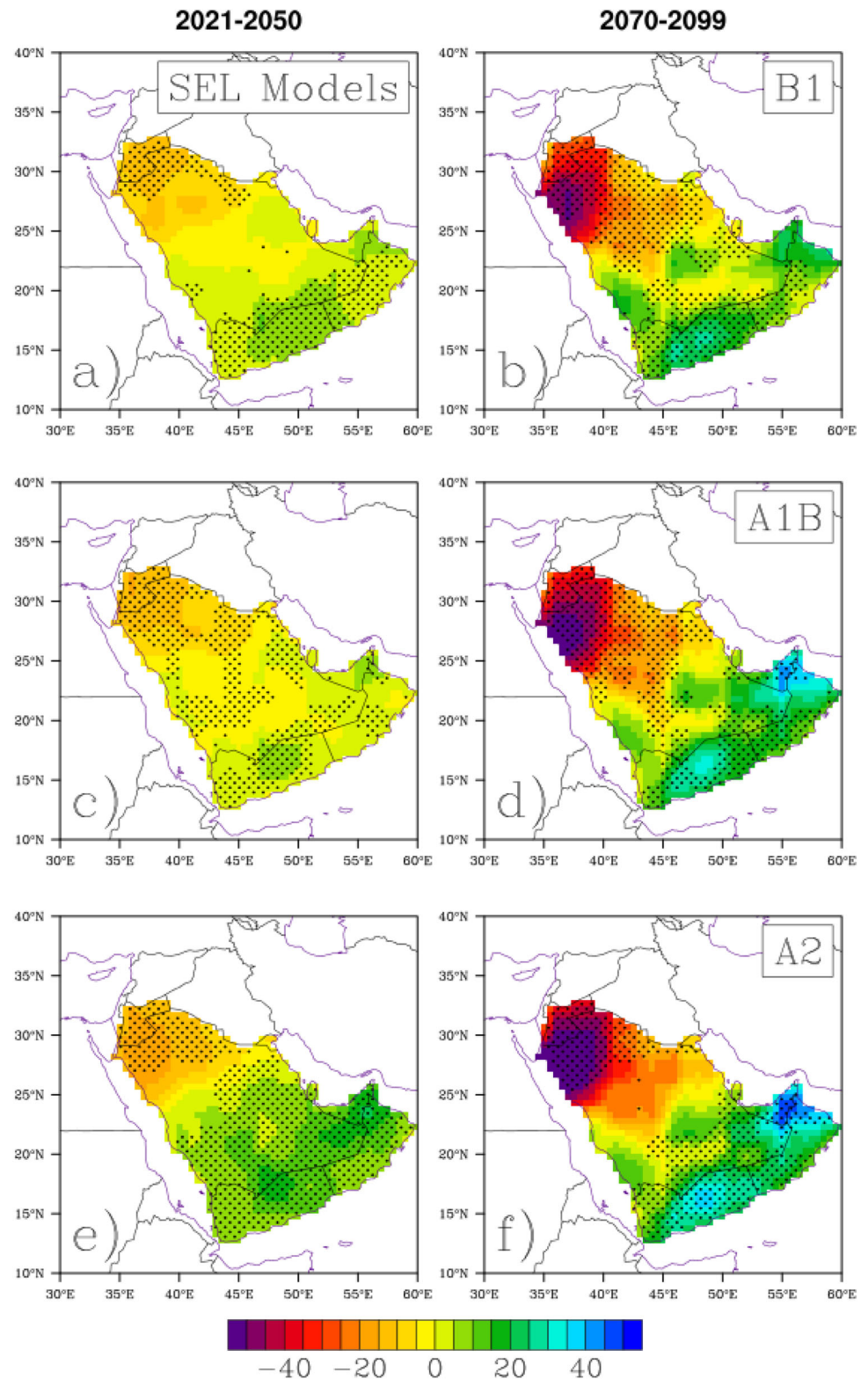
Fig. 9 Future changes in all (22 CMIP3) models ensemble mean precipitation (in %) for near (2021–2050, *left panel*) and far (2070–2099, *right panel*) with reference to the base period (1970–1999). Dotted areas indicate regions where at least 66% of CMIP3 models agree on sign of future changes signals of precipitation over the Arabian Peninsula. The SRES scenarios are B1 (*top*), A1B (*middle*), and A2 (*bottom*)



precipitation over the Arabian Peninsula does not show any clear increasing trend, but a strong interannual variability can be seen over the entire period of integration. The interannual variability is larger in the all models (Fig. 13a)

compared to the best performing models (Fig. 13b). However, the spread associated with intermodel STD and intermodel range is reduced remarkably for the best performing models compared to the all models (Fig. 13c, d).

Fig. 10 Same as Fig. 9 except for the best performing models



The Box-and-Whisker plot shows that MME mean precipitation increases as a result of global warming in the 21st century, with the greatest increases under A2 (Fig. 14). The uncertainty in precipitation projection

increases with integration of time and emissions scenario from lower range to higher range. By the end of the 21st century, the annual mean precipitation seems to be increased by 5.16 ± 30 , 10.48 ± 34 , and $15.29 \pm 43\%$,

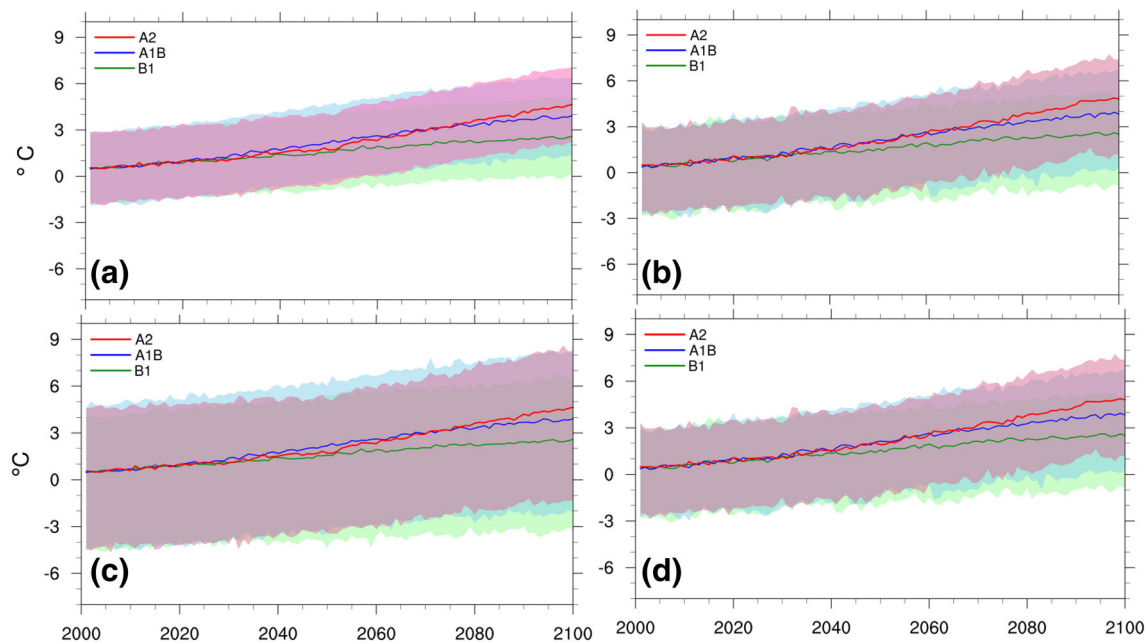


Fig. 11 **a** Annual mean temperature anomalies (unit: °C) averaged over the Arabian Peninsula, relative to 1970–1999 for B1 (green), A1B (blue), and A2 (red) scenarios from the MME mean (solid line) with ± 1 intermodel standard deviation (color shading). The ± 1

intermodel standard deviation for B1, A1B, and A2 scenarios are shown by pale green, sky blue, and violet red colors. **b** Same as **a** except for best performing models. **c–d** is same as **a**, **b** except the shading shows the intermodel range (see text for further explanation)

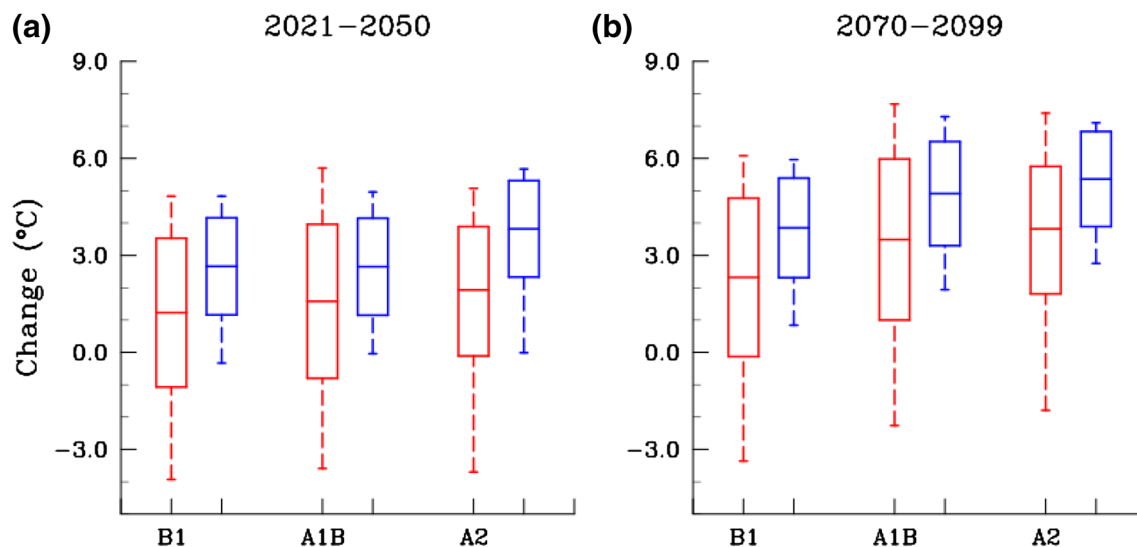


Fig. 12 Box-and-Whisker plots show the domain averaged temperature change over the Arabian Peninsula for the future periods **a** 2021–2050 and **b** 2070–2099 w.r.t. the base period 1970–1999 for all models (red) and best performing models (blue). The band in the box represents the change in MME mean; the bottom (top) of the box

represents the MME mean SAT change ± 1 intermodel standard deviation. The ends of the Whiskers represent the intermodel range, i.e., multi-model maximum and minimum change w.r.t base period MME mean simulation values

relative to the present climate, under the B1, A1B, and A2 scenarios, respectively, for all models, and it is 3.2 ± 25 , 1.82 ± 28 , and $5.3 \pm 32\%$ for best performing models (Fig. 14b). For all models, the intermodel range of projected precipitation varies widely from -94 to 265 , -95 to 322 , and -95 to 375% for the B1, A1B, and A2 scenarios,

respectively, and it is -71 to 175 , -74 to 205 , and -75 to 235% , respectively, for best performing models (Fig. 14b). Contrary to the all models, the intermodel range for the best performing models shows less scenario dependence (Fig. 14). By the end of 21st century an increase MME mean precipitation can be seen in the A2 scenario for both

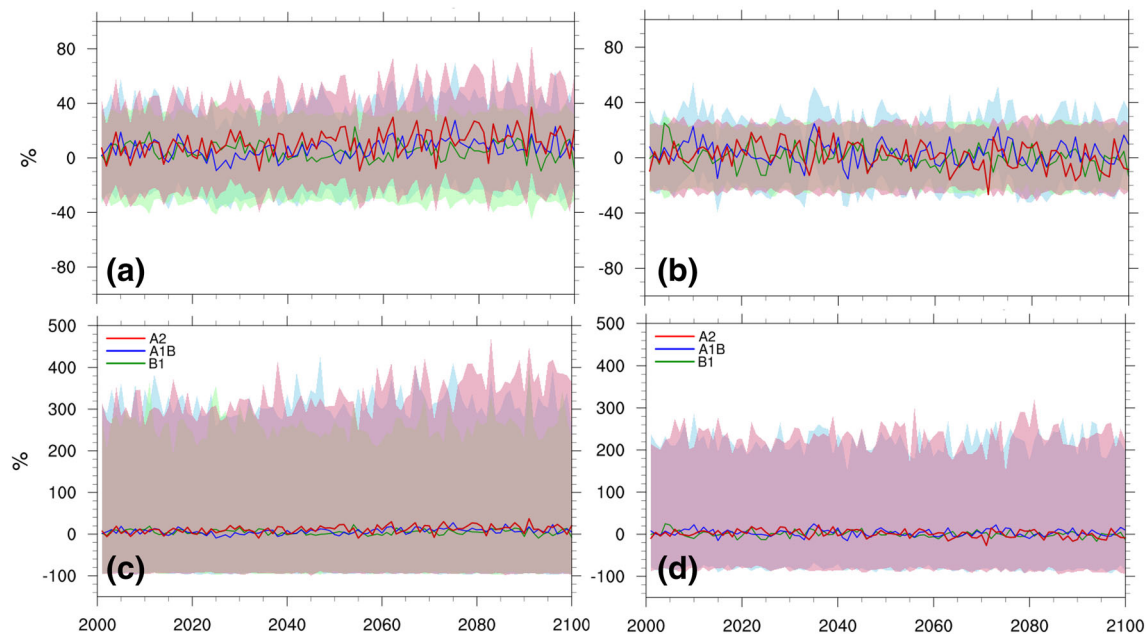


Fig. 13 Same as Fig. 11 except for precipitation (%)

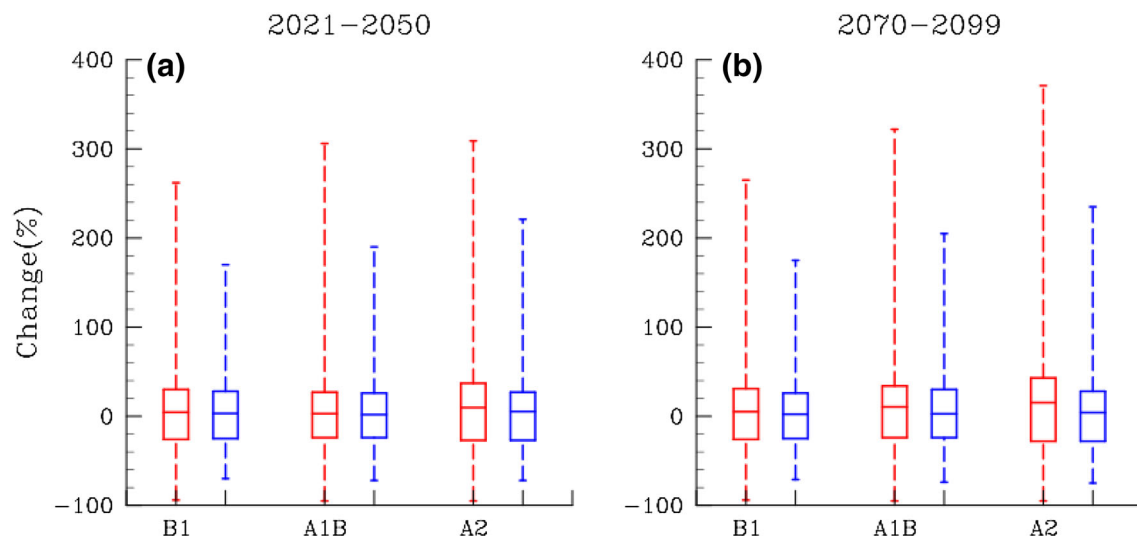


Fig. 14 Same as Fig. 12 except for precipitation (%). The band in the box represents the change in the MME mean; the bottom (top) of the box represents the MME mean change ± 1 intermodel standard

best performing and all models. In comparison with the temperature, the increasing rate in precipitation during the 21st century is smaller, but with a larger uncertainty in its projection.

Although there is no guarantee that the nature of the present day climate will be continued to the projection period (Reichler and Kim 2008; Reifen and Toumi 2009), however, comparison of model data with the base period observation is commonly used technique for screening good performing models over a particular region. Model projected temperature and precipitation are not free from

deviation. The ends of the whiskers represent the intermodel range, i.e., multi-model maximum and minimum change w.r.t base period MME mean simulation values

uncertainties whatever the category they are in, however, corrected (projected plus the bias in base period) values of the parameters may provide reasonable estimates for long-term planning. Figure 15 shows the corrected temperature for the B1, A1B, and A2 scenarios for both all and best performing models. In case of B1 and A2 scenarios, the south and southeastern (northwestern) parts of the Arabian Peninsula are expected to receive higher (lower) temperature in future, whereas for A1B scenario, the wider east-west belt is expected to receive higher annual mean temperature. Similar to temperature, the precipitation also

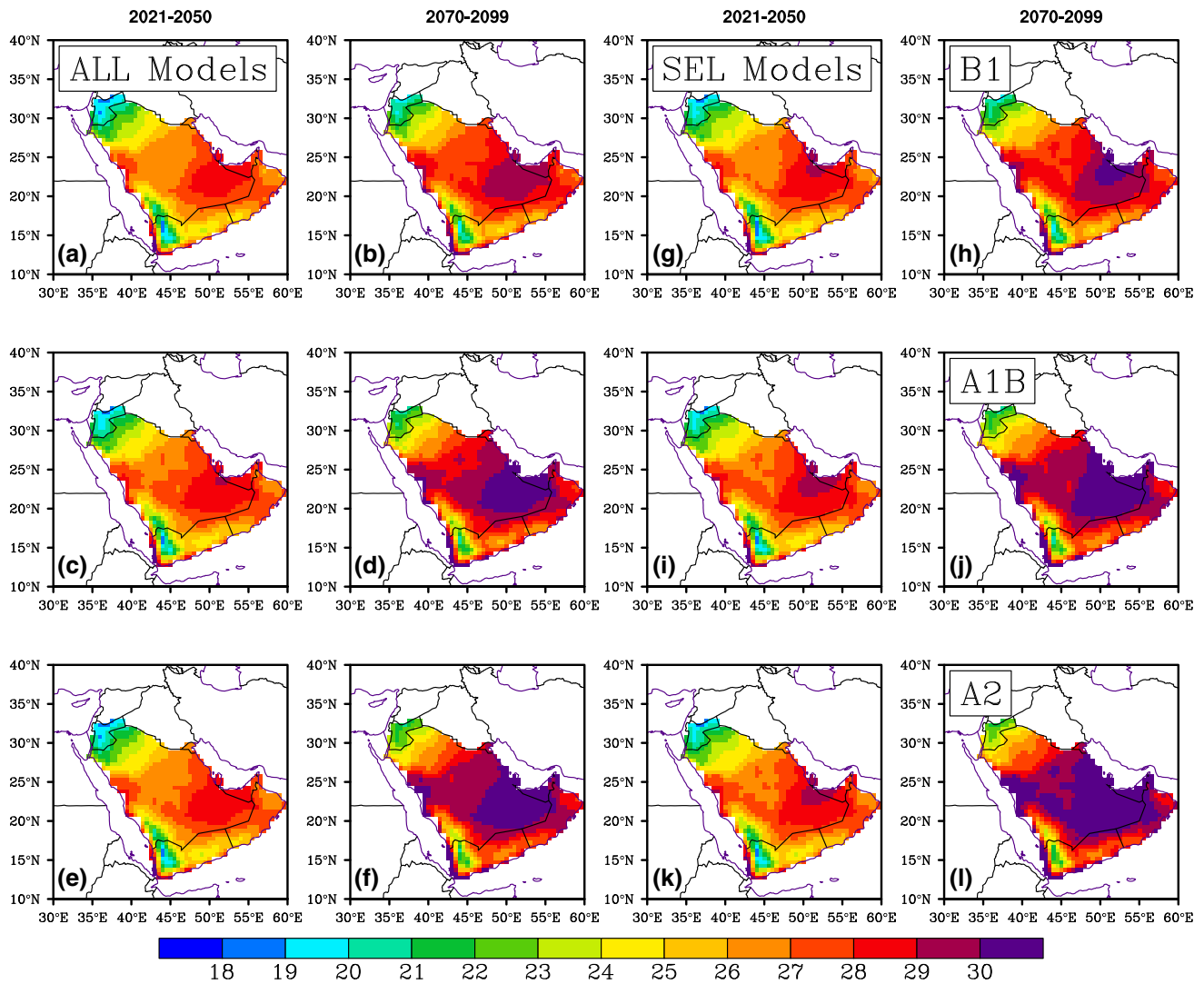


Fig. 15 MME mean corrected future temperature (units: °C) for all models (*first and second columns*) and selected best performing models (*third and fourth columns*)

displays homogenous pattern for B1, A1B, and A2 scenarios with more increase in the southern and southeastern sides and less towards the north and northwestern sides. Compared to the projected temperature and precipitation values (Figure S1; Figure S2), the corrected temperature and precipitation (Figs. 15, 16) show nearly similar spatial distribution with slight differences in magnitude. These results may verify with the newly developed SAUDI-KAU coupled global climate model (Almazroui et al. 2017) simulations with high resolutions in the future study.

4 Summary and conclusions

In this study, we categorized the 22 CMIP3 models into four groups based on their performance in the present day climate (1970–1999) climate and examined the

uncertainties associated with future projection of annual mean surface air temperature and precipitation over the Arabian Peninsula under SRES B1, A1B, and A2 scenarios. Based on our analysis, the CMIP3 models are grouped into the following four categories, namely (1) all models, (2) precipitation-based models, (3) temperature-based models, and (4) best performing models. Out of these four categories, the models in group (1) and (4) are used for the assessment of uncertainties in future projections of annual mean temperature and precipitation over the Arabian Peninsula. The fourth category of models, i.e., the best performing models, revealed the lowest multi-model ensemble (MME) mean bias and the intermodel standard deviation values for surface air temperature and precipitation over the peninsula compared to the first three categories. The best performing models not only reproduce well the annual cycle of temperature and precipitation but

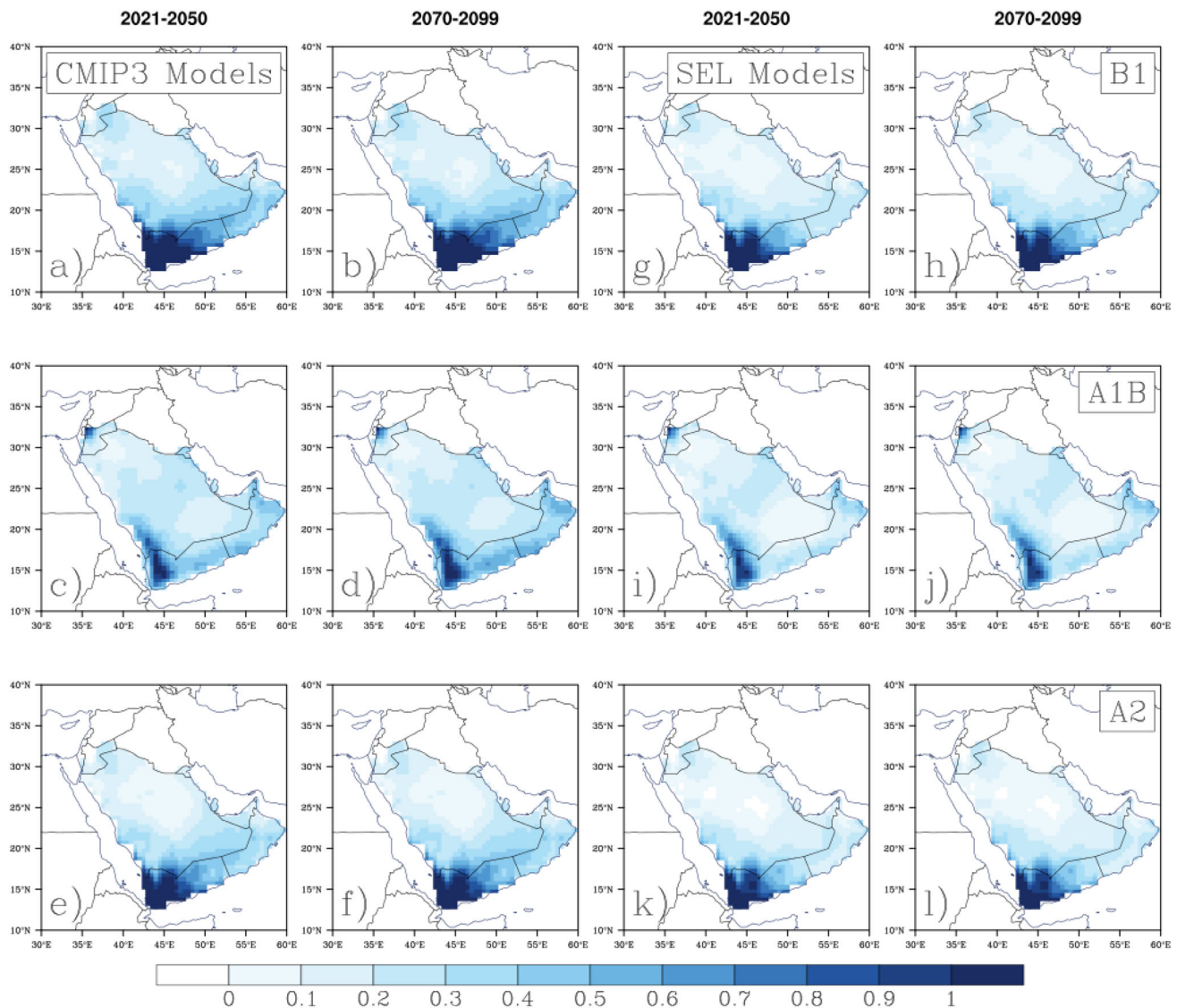


Fig. 16 Same as Fig. 15 except for precipitation (mm/day)

also display lowest systematic error, NRMSE, and standard error compared to the observations.

The analysis of future simulations revealed a continuous increase in temperature over the Arabian Peninsula during the 21st century. For the period 2070–2099, the temperature is projected to increase by 2.32 ± 2.45 , 3.49 ± 2.49 , and 3.28 ± 1.47 °C, relative to the present day climate, under the SRES B1, A1B, and A2 scenarios, respectively, while the intermodel ranges are projected to be from -3.36 to 6.08 , -2.26 to 7.68 , and -1.79 to 7.40 °C, respectively. The best performing models remarkably reduced the uncertainties in temperature projections where annual mean temperature is increased by 3.85 ± 1.54 , 4.91 ± 1.61 , and 5.36 ± 1.47 °C, relative to the present climate, under the B1, A1B, and A2 scenarios, respectively; and the intermodel ranges are projected to be from

0.84 to 5.96 , 1.94 to 7.29 and 2.75 to 7.10 °C, respectively. Spatially, the annual mean temperature shows a homogeneous warming pattern across the Arabian Peninsula. The warming rate is increasing more from central to the northern parts of the peninsula. Meanwhile, for the period 2070–2099, the annual mean precipitation is projected to increase by 5.16 ± 30 , 10.48 ± 34 , and $15.29 \pm 43\%$, relative to the present climate, under the B1, A1B, and A2 scenarios, respectively, while the intermodel ranges are projected to be from -94 to 265 , -95 to 322 , and -95 to 375% , respectively, for all models. The best performing models slightly reduced the precipitation uncertainty band with MME mean projected to increase by 3.2 ± 25 , 1.82 ± 28 , and $5.3 \pm 32\%$, relative to the present day climate, under the B1, A1B, and A2 scenarios, respectively, while the intermodel ranges are projected to be from

−71 to 175, −74 to 205, and −75 to 235%, respectively. Although at a low confidence level (at least 66% of model agree in sign of change), a homogeneous wetting (drying) pattern is projected across southern and eastern (north-western) parts of the Arabian Peninsula at annual scale, with a larger increase at the end of 21st century.

Although, the projected changes in the temperature and precipitation by the 22 CMIP3 models over the Arabian Peninsula closely resemble to those shown by Almazroui et al. (2016), but the present study further indicates that a better choice of models from the CMIPs (e.g. CMIP3 and CMIP5) could reduce the uncertainty range associated with the future projections of temperature and precipitation over the Arabian Peninsula. Following above results, we plan another study to examine the projected future changes and associated uncertainties in the temperature and precipitation simulated by different categories of CMIP5 models over the Arabian Peninsula. For climate change impact assessments, the potential inputs with reduced uncertainty range in future projections may help the policy makers to address better the climate-related threats in the Arabian Peninsula.

Acknowledgements This project was funded by the King Abdulaziz City for Science and Technology, award number AT-35-205. The ICTP, Trieste, Italy, is acknowledged for providing CMIP3 data. Computation for the work described in this paper was performed using the Aziz Supercomputer at King Abdulaziz University's High Performance Computing Center, Jeddah, Saudi Arabia.

Open Access This article is distributed under the terms of the Creative Commons Attribution 4.0 International License (<http://creativecommons.org/licenses/by/4.0/>), which permits unrestricted use, distribution, and reproduction in any medium, provided you give appropriate credit to the original author(s) and the source, provide a link to the Creative Commons license, and indicate if changes were made.

References

- Almazroui M (2011) Calibration of TRMM rainfall climatology over Saudi Arabia during 1998–2009. *Atmos Res* 99:400–414. doi:10.1016/j.atmosres.2010.11.006
- Almazroui M, Islam MN, Athar H, Jones PD, Rahman MA (2012a) Recent climate change in the Arabian Peninsula: annual rainfall and temperature analysis of Saudi Arabia for 1978–2009. *Int J Climatol* 32:953–966. doi:10.1002/joc.3446
- Almazroui M, Islam MN, Jones PD, Rahman MA (2012b) Recent climate change in the Arabian Peninsula: seasonal rainfall and temperature climatology of Saudi Arabia for 1979–2009. *Atmos Res* 111:29–45
- Almazroui M, Abid MA, Athar H, Islam MN, Ehsan MA (2013) Interannual variability of rainfall over the Arabian Peninsula using the IPCC AR4 Global Climate Models. *Int J Climatol* 33:2328–2340. doi:10.1002/joc.3600
- Almazroui M, Islam MN, Dambul R, Jones PD (2014) Trends of temperature extremes in Saudi Arabia. *Int J Climatol* 34:808–826
- Almazroui M, Saeed F, Islam MN, Al-Khalaf AK (2016) Assessing the robustness and uncertainties of projected changes in temperature and precipitation in AR4 Global Climate Models over the Arabian Peninsula. *Atmos Res* 15:163–175
- Almazroui M, Tayeb O, Mashat AS, Yousef A, Al-Turki YA, Abid MA, Bafail AO, Ehsan MA, Zahed A, Rahman MA, Mohorji AM, Kang IS, Noaman A, Omar M, Al-roqi AM, Ammar K, Al-Ghamdi AS, Hussein MA, Katib I, O'Brien E, Aljohani NR, Islam MN, Alsaedi A, Yang YM, Alkhalaf AK, Ismail M, Mashat A, Kucharski F, Assiri M, Ibrahim S, Tippet M, Rashid IU, Kamil S, Alahmadi A, Atif RM, Bajunaid MA, Hantoush AS (2017) Saudi-KAU coupled global climate model: description and performance. *Earth Syst Environ* 1(1). doi:10.1007/s41748-017-0009-7
- AlSarmi SH, Washington R (2011) Recent observed climate change over the Arabian Peninsula. *J Geophys Res* 116:D11. doi:10.1029/2010JD015459
- AlSarmi SH, Washington R (2013) Changes in climate extremes in the Arabian Peninsula: analysis of daily data. *Int J Climatol* 34:1329–1345. doi:10.1002/joc.3772
- Barfus K, Bernhofer C (2014) Assessment of GCM performances for the Arabian Peninsula, Brazil, and Ukraine and indications of regional climate change. Advance online publication. *Environ Earth Sci* 72(12):1–15. doi:10.1007/s12665-014-3147-3
- Biasutti M, Held IM, Sobel AH, Giannini A (2008) SST forcings of Sahel rainfall variability in simulations of the 20th and 21st centuries. *J Clim* 21:3471–3486. doi:10.1175/2007JCLI1896.1
- Chakraborty A, Behera SK, Mujumdar M, Ohba R, Yamagata T (2006) Diagnosis of tropospheric moisture over Saudi Arabia and influences of IOD and ENSO. *Mon Weather Rev* 134:598–617
- Daron JD, Sutherland K, Jack C, Hewitson BC (2014) The role of regional climate projections in managing complex socio-ecological systems. *Reg Environ Change* 15:1–12. doi:10.1007/s10113-014-0631-y
- Deng L, McCabe MF, Stenchikov G, Evans J, Kucera P (2015) Simulation of flash-flood producing storm events in Saudi Arabia using the Weather Research and Forecasting model. *J Hydrometeorol* doi:doi. doi:10.1175/JHM-D-14-0126.1
- Donat MG, Peterson TC, Brunet M, King AD, Almazroui M, Kolli RK, Boucherf D, Al-Mulla AY, Nour AY, Aly AA, Nada TAA, Semawi MM, Al Dashti HA, Salhab TG, El Fadli KI, Muftah MK, Dah Eida S, Badi W, Driouech F, El Rhaz K, Abubaker MJY, Ghulam AS, Erayah AS, Mansour MB, Alabdouli WO, Al Dhanhani JS, Al Shekaili MN (2014) Changes in extreme temperature and precipitation in the Arab region: long-term trends and variability related to ENSO and NAO. *Int J Climatol* 34:581–592. doi:10.1002/joc.3707
- El Kenawy AM, Stenchikov GL, Raj J (2014) Multi-decadal classification of synoptic weather types, observed trends and links to rainfall characteristics over Saudi Arabia. *Front Environ Sci* 2:37. doi:10.3389/fenvs.2014.00037
- Evans JP (2009) 21st century climate change in the Middle East. *Clim Change* 92:417–432
- Haensler A, Saeed F, Jacob D (2013a) Assessing the robustness of projected precipitation changes over central Africa on the basis of a multitude of global and regional climate projections. *Clim Change* 121:349–363. doi:10.1007/s10584-013-0863-8
- Haensler A, Saeed F, Jacob D (2013b) Assessment of projected climate change signals over central Africa based on a multitude of global and regional climate projections. In: Haensler A, Jacob D, Kabat P, Ludwig F (eds) *Climate change scenarios for the Congo Basin*. Climate Service Centre Report 459 No. 11, Hamburg, Germany (ISSN: 460 2192-4058)
- Hallegatte S (2009) Strategies to adapt to an uncertain climate change. *Glob Environ Chang* 19(2):240–247

- Hawkins E, Sutton R (2009) The potential to narrow uncertainty in regional climate predictions. *Bull Am Meteorol Soc*. doi:[10.1175/2009BAMS2607.1](https://doi.org/10.1175/2009BAMS2607.1)
- IPCC (2000) A special report of IPCC working group III, Summary for policymakers, published for the intergovernmental panel on climate change. ISBN: 92-9169-113-5. Available at <https://ipcc.ch/pdf/specialreports/spm/sres-en.pdf>
- Islam MN (2009) Rainfall and temperature scenario for Bangladesh. *Open Atmos Sci J* 3:93–103
- Islam MN, Uyeda H (2007) Use of TRMM in determining the climatic characteristics of rainfall over Bangladesh. *Remot Sens Environ* 108(3):264–276. doi:[10.1016/j.rse.2006.11.011](https://doi.org/10.1016/j.rse.2006.11.011)
- Islam MN, Rafiuddin M, Ahmed AU, Kolli RK (2008) Calibration of PRECIS in employing future scenarios in Bangladesh. *Int J Climatol* 28:617–628
- Kendall MG (1976) *Rank Correlation Methods*. 4th Ed. Griffin
- Kwarteng AY, Dorvlo AS, Kumar GTV (2009) Analysis of a 27-year rainfall data (1977–2003) in the Sultanate of Oman. *Int J Climatol* 29:605–617. doi:[10.1002/joc.1727](https://doi.org/10.1002/joc.1727)
- Meehl GA, Arblaster JM, Tebaldi C (2005) Understanding future patterns of increased precipitation intensity in climate model simulations. *Geophys Res Lett* 32:L18719. doi:[10.1029/2005GL023680](https://doi.org/10.1029/2005GL023680)
- Meehl GA, Covey C, Taylor KE, Delworth T, Stouffer RJ, Latif M, McAvaney B, Mitchell JF (2007) The WCRP CMIP3 multimodel dataset: a new era in climate change research. *Bull Am Meteorol Soc* 88(9):1383–1394
- Mitchell TD, Jones PD (2005) An improved method of constructing a database of monthly climate observations and associated high resolution grids. *Int J Climatol* 25:693–712. doi:[10.1002/joc.1181](https://doi.org/10.1002/joc.1181)
- New M, Hulme M, Jones P (2000) Representing twentieth century space time climate variability. Part II: development of 1901–1996 monthly grids of terrestrial surface climate. *J Clim* 13(13):2217–2238
- Reichler T, Kim J (2008) How well do coupled models simulate today's climate? *Bull Am Meteorol Soc*. doi:[10.1175/BAMS-89-3-303](https://doi.org/10.1175/BAMS-89-3-303)
- Reifen C, Toumi R (2009) Climate projections: past performance no guarantee of future skill? *Geophys Res Lett* 39:L13704. doi:[10.1029/2009GL038082](https://doi.org/10.1029/2009GL038082)
- Solomon S, Qin D, Manning M, Chen Z, Marquis M, Averyt K, Tignor M, Miller H (eds) (2007) *Contribution of working group I to the fourth assessment report of the intergovernmental panel on climate change*. Cambridge University Press, Cambridge
- Whetton P, Hennessy K, Clarke J et al (2012) Use of representative climate futures in impact and adaptation assessment. *Clim Change* 115(3–4):433–442. doi:[10.1007/s10584-012-0471-z](https://doi.org/10.1007/s10584-012-0471-z)